# Optical and electrical properties of Pbs + In thin films subjected to thermal processing

R.S. Parra*, P.J. George[1], G.G. Sánchez, A.E. Jiménez González, L. Baños[2], P.K. Nair

*Centro de Investigación en Energía, Universidad Nacional Autónoma de México, Temixco, Morelos 62580, Mexico*

## Abstract

Indium thin film ($\sim 20$ nm) deposited on intrinsic lead sulfide films leads to the formation of an n-type composite layer when annealed in nitrogen atmosphere at 350–400°C. The formation of metallic lead and indium oxide is observed in the X-ray diffraction patterns of the films. The dark conductivity of the PbS + In films after nitrogen annealing at 400°C attains a value of $500 \ \Omega^{-1} \ cm^{-1}$, which is higher by five orders of magnitude compared with as-prepared PbS films. Modifications in the optical and electrical properties of PbS + In films after annealing are attributed to the presence of metallic lead and indium oxide in the films. © 2000 Elsevier Science Ltd. All rights reserved.

*Keywords*: Indium; A. Thin films; D. Optical properties; D. Electrical properties

## 1. Introduction

In recent papers, we reported on the structural, electrical and optical properties of annealed CdS [1], CdSe [2,3] and $Bi_2S_3$ [4] thin films incorporating a thin film of metallic indium. The annealing process at 250 to 400°C, in air and nitrogen brought about substantial modifications in the properties of the base thin film. In the case of CdS and CdSe thin films, heterostructures of the type CdS:In–$In_2O_3$ or CdSe:In–$In_2O_3$ has been produced with a relatively high electrical conductivity for the underlying cadmiun chalcogenide film, compared with the near intrinsic conductivity of the as deposited film. And annealing process of $Bi_2S_3$ films with a metallic indium film led to the formation of a composite of the type $Bi_2S_3$–Bi:$In_2O_3$ again with a relatively high electrical conductivity for the underlying film.

In the present work, we report on the crystalline structure, composition as well as on the major features in the optical and electrical properties of a composite film: PbS–Pb:$In_2O_3$. Interest in lead chalcogenide thin films is mainly based on the infrared photosensitivity of $PbS_{1-x}Se_x$, $PbSe_{1-x}Te_x$ [5]. Later on PbS thin films have been considered for their suitability for photothermal and thermophotovoltaic conversion of solar energy [6–11]. Latest addition to the application of PbS is in solar radiation control coatings of PbS–CuS [12,13].

In the present work PbS thin films were prepared by chemical bath deposition technique [14]. During the formation of lead sulfide films by the technique of chemical bath deposition, the possible inclusion of hydroxo anions or molecules of water in the structure of the film have been reported previously [15,16]. However, techniques to remove these components from the film have not been studied. In this work, we proposed the use of metallic indium film to react with chemisorbed oxygen, hydroxo anions or molecules of water incorporated in the films, to prevent the formation of lead oxo-sulfates when annealing at temperatures above 300°C. However, we noted that the annealing produced metallic lead converting the base film into a composite, rather than leading to higher photosensitivity.

## 2. Experimental details

Thin films of PbS were deposited on corning glass

* Corresponding author.

*E-mail address:* rsp@mazatl.cie.unam.mx (R.S. Parra).

[1] Permanent address: Department of Electronic Science, Kurukshetra University, Kurukshetra, Haryana 132119, India.

[2] Departamento de Materiales Metálicos y Cerámicos, IIM-UNAM, Circuito Exterior C. Universitaria, México D.F., c.p. 04510, apdo. p. 70-360.
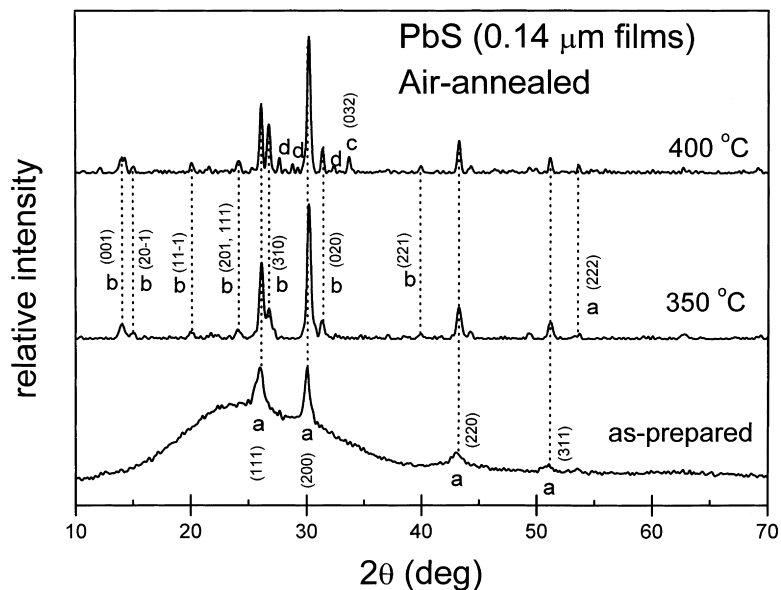
Fig. 1. X-ray diffraction patterns (Cu-K$_\alpha$) of PbS thin films: as-prepared and air-annealed at 350 and 400°C. Galena peaks (a-peaks JCPDS 5-0592) are dominant, and small peaks of lead oxo-sulfates (b-peaks JCPDS 33-1486 and c-peak JCPDS 23-0333) and lead hydroxide (d-peaks JCPDS 11-0270) are observable in the diffractograms of films air-annealed above 300°C.

substrates (75 × 25 mm and 1 mm thick) by immersing them into the chemical bath. The glass substrates were cleaned in sulfuric acid for 24 h to remove organic matter and then were washed in a solution of commercial detergent powder, rinsed in deionized water and dried. The chemical bath was prepared by mixing 2.5 ml of 1 M lead acetate solution, 10 ml of 1 M NaOH solution, 6.0 ml of 1 M thiourea solution and 2 ml of 1 M triethanolamine solution. The volume was adjusted to 100 ml with deionized water. Baker Analyzed Reagents were used in this work. The PbS films were deposited for 1.5, 2 and 3 h at room temperature (24–26°C). After deposition, the films were washed in deionized water and dried in hot air. Immediately after a thin film of about 20 nm thickness of metallic indium was deposited on the film by evaporating indium of 99.999% purity (Alfa Products) in a vacuum chamber evacuated to $10^{-6}$ torr. The PbS and PbS + In films were air- and nitrogen-annealed at 350 and 400°C for 1 h each, at atmospheric pressure, in a tubular furnace.

Measurements of the dark- and photo-current of the films were made using a Keithley 619 multimeter and a Keithley 230 programmable voltage source. For this, coplanar silver print electrodes (5-mm long, 5-mm separation) were painted over the film surface after subjecting them to the annealing process mentioned before. A 250 W tungsten–halogen lamp was used as the illumination source, which produced at the plane of the film an intensity of illumination of 2000 W m$^{-2}$. The applied bias was 0.1 V in all cases.

X-ray diffraction (XRD) patterns of PbS + In films were recorded on a Siemens D 500 system using (CuK$_\alpha$) radiation. The diffraction patterns of PbS and PbS + In films showed peaks superimposed on the background pattern of the glass substrate. In general, this background was subtracted from the total spectra to prepare the figs. A Siemens SRS 300 X-ray fluorescence (XRF) spectrometer was used to determine the presence of indium, lead and sulfur in the PbS + In films. The XRF spectra were recorded using a LiF (110) crystal, ($2d = 0.2848$ nm) for Pb-L$_\alpha$ fluorescence line ($2\theta = 48.73°$), LiF (100) crystal, ($2d = 0.4027$ nm) for In-L$_{\alpha 1}$ fluorescence line ($2\theta = 139°$) and a Pentaerythrite crystal ($2d = 0.8742$ nm) for S-K$_{\alpha 1,2}$ fluorescence line ($2\theta = 75.85°$).

Optical transmittance and specular reflectance spectra of as-prepared and annealed films were recorded on a Shimadzu UV-VIS-NIR 3101 PC Spectrophotometer.

Film thickness was determined using Alpha-step 100 step thickness measuring equipment (Tencore Instruments, USA). For PbS films, deposited in a time of 1.5, 2 and 3 h, the thickness was found to be (0.12 ± 0.01; 0.14 ± 0.01 and 0.17 ± 0.01) μm, respectively. For PbS + In films the total thickness was estimated to be higher on an average by 0.02 μm.

The structural, electrical and optical properties of PbS and PbS + In films were studied in detail in films deposited in 2 h (~0.14 μm thickness).

## 3. Results and discussion

### 3.1. Structural analysis

Fig. 1 shows the XRD patterns of PbS films deposited on glass substrates, as-prepared and air-annealed at 350 and

Table 1
Grain size, in Å, of lead sulfide, metallic indium and metallic lead in single PbS and in composite PbS + In films. The calculation was done using the Scherrer formula [17]. The (111) and (200) reflections were located at $2\theta \cong 26°$ and $2\theta \cong 30°$ for PbS; (101) reflection located at $2\theta \cong 33°$ for metallic indium and (111) and (200) reflections were located at $2\theta \cong 31°$ and $2\theta \cong 36°$ for metallic lead

| | PbS film | | PbS–In film[a] | Pb | | In film | PbS–In film[a] |
|---|---|---|---|---|---|---|---|
| As-prepared grain size (Å) | 130 | | 120 | | | 300 | 200 |
| Air annealed at: | 350°C | 400°C | | There is no formation of Pb | | | |
| Grain size (Å) | 200 | 260 | – | | | – | – |
| N₂ annealed at: | 350°C | 400°C | | 350°C | 400°C | | There are no peaks of In. |
| Grain size (Å) | 180 | 180 | There are no peaks of PbS | 160 | 160 | – | |

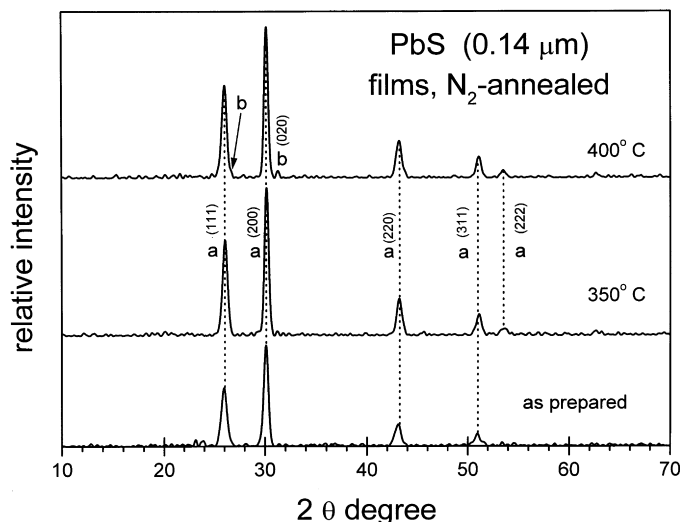[a] PbS and metallic In peaks measured in composite film.

Fig. 2. X-ray diffraction patterns (Cu-K$_\alpha$) of PbS thin films: as-prepared and nitrogen-annealed at 350 and 400°C. A small peak of lead oxosulfate at $2\theta \cong 31°$ is still seen (b-peak JCPDS 33-1486) when films are annealed at 400°C.

400°C. The as-prepared PbS film presents the (111), (200), (220) and (311) peaks corresponding to its rocksalt structure PbS-Galena (JCPDS 5-0592) superimposed on the background due to glass substrate. The diffractograms of air-annealed PbS films show an increase in the relative intensity of the characteristic galena peaks (a-peaks); the grain size, calculated using Scherrer formula [17], is increased as seen in Table 1. However, these diffractograms indicate the presence of lead oxide sulfates (JCPDS 33-1486, b-peaks) in the case of air-annealed films at 350°C. Lead oxide sulfate (JCPDS 23-0333, c-peak) and lead hydroxide (JCPDS

11-0270, d-peaks) are noticed in samples air-annealed at 400°C.

Fig. 2 shows the XRD patterns of PbS films nitrogen-annealed at 350 and 400°C as well as that of the as-prepared film. The size of PbS crystallites of nitrogen-annealed (for 1 h) films is almost the same as that of the PbS crystallites in the as-prepared films, see Table 1. The XRD patterns of nitrogen-annealed PbS films exhibit good agreement with the standard XRD pattern of galena. However, the formation of lead oxide sulfate (b-peak) is detected in the diffractograms of the film baked at 400°C.
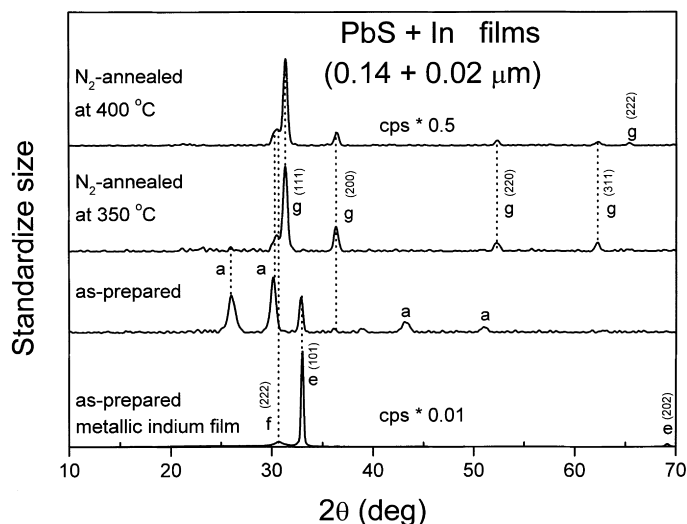


Fig. 3. X-ray diffraction patterns of PbS + In films, as-prepared and nitrogen-annealed at 350 and 400°C. X-ray diffraction patterns of metallic indium film are presented too. The presence of metallic indium (JCPDS 5-0642) and galena are well noted in the as-prepared film. In the case of annealed films the presence of metallic lead is not seen.
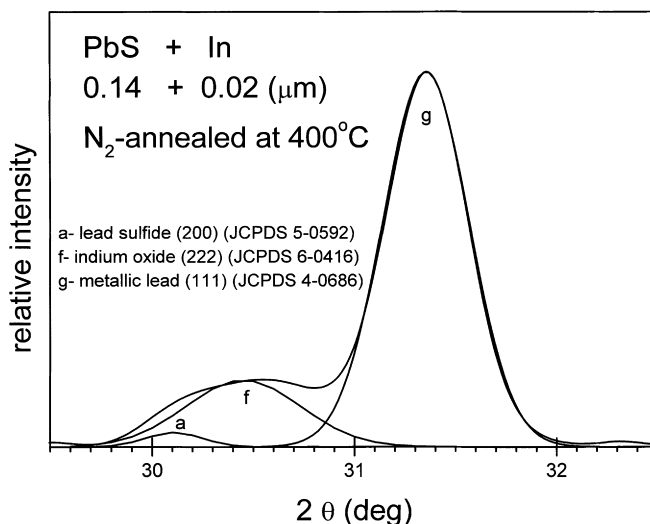
Fig. 4. Resolution of composite peak in the interval $2\theta \cong 29.7$–$31.2°$. This figure shows that the peak is formed by galena and indium oxide.

The XRD analysis of air-annealed PbS films, prepared at temperatures above 300°C, confirmed that the initial composition of the semiconductor film is changed; the formation of lead oxo-sulfates is clearly seen. Although nitrogen-annealing process inhibits the formation of lead oxo-sulfates and lead hydroxide in the PbS film, the presence of lead oxo-sulfate is not eliminated, completely when annealed at 400°C.

Fig. 3 shows XRD patterns of PbS + In films subjected to nitrogen annealing. For comparison the XRD patterns of the as-prepared indium film (20 nm) on glass substrate is also given in Fig. 3.

The diffractogram of metallic indium shows two peaks: at $2\theta \cong 33°$ for (101) planes and at $2\theta \cong 69°$ for (202) planes

in accordance with JCPDS 5-0642. High relative intensity of the metallic indium peaks is related to good crystallinity on the surface of glass substrate. In this film, the presence of indium oxide is detected through the presence of a peak at $2\theta \cong 30.6°$ for (222) planes, which produce the most intense reflection for $In_2O_3$ (JCPDS 6-0416).

In the XRD patterns of as-prepared PbS + In film only the major metallic indium peak at $2\theta \cong 33°$ for (101) planes is observed. Assuming that recently evaporated indium film did not come into the bulk of lead sulfide film, we could interpret that the relatively low intensity of indium peak is due to inferior crystallinity of indium over the film of PbS. Another explanation for the relatively low intensity of
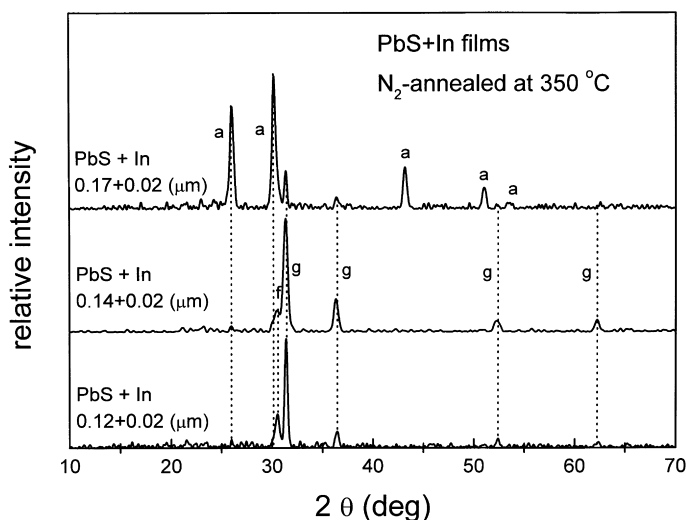


Fig. 5. Comparison of XRD diffraction patterns of composite films with different duration of deposition time for PbS, and nitrogen-annealed at 350°C. Thickness of metallic indium was the same in all the films.
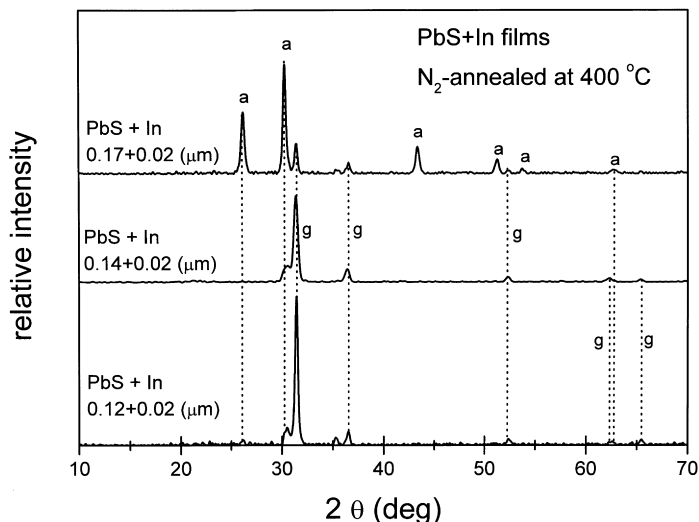
Fig. 6. Comparison of XRD diffraction patterns of composite films with different duration of deposition time for PbS, and nitrogen-annealed at 400°C. Thickness of metallic indium was the same in all the films.

indium peak may be that indium diffuses into the bulk of the PbS film, during the evaporation which would result in smaller film thickness for metallic indium. As we can see in Table 1, the size of crystallites in evaporated indium over a lead sulfide film is one- third that in evaporated indium film on a glass substrate. Here, the change in the crystallite size of indium supports the idea of indium diffusion into the PbS film.

After annealing PbS + In films in nitrogen at 350 or 400°C, they show modifications in the XRD patterns. These diffractograms are dominated by the presence of metallic lead peaks (g) in the positions $2\theta \cong 31.3°$, 36.2°, 52.2° and 62.1°. The presence of a composite peak at $2\theta \cong 30.5°$ is noticed. The absence of metallic indium and galena peaks is a major feature of the nitrogen annealed PbS + In films. The grain size of metallic indium deposited and metallic lead formed during the annealing is given in Table 1. A gaussian regression analysis of the composite peak near $2\theta \cong 30.5°$, shown in Fig. 4, demonstrates that PbS (200) reflection at $2\theta \cong 30.1°$, and $In_2O_3$ (222) reflection at $2\theta \cong 30.5°$ constitute this peak.

The presence of the indium oxide peak suggests that during the annealing process indium reacts with chemisorbed oxygen available from the air in the intergrain region of PbS and with $Pb(OH)_2$ trapped in the film.

To have complementary information about the structural changes promoted by indium in PbS during nitrogen annealing at 350 or 400°C, PbS + In films with different PbS film thickness were prepared. Thickness of the PbS films was varied using different duration of deposition, 1.5 h (0.12 μm), 2 h (0.14 μm) and 3 h (0.17 μm), in the chemical bath. Thickness of evaporated indium film, on PbS films, was approximately same 20 nm, in the three cases.

The Figs. 5 and 6, show the influence of metallic indium in the films with different thickness of PbS. After nitrogen-annealing it is seen that in PbS films, of 0.12 and 0.14 μm of thickness, metallic indium led to the formation of indium oxide (peak f), present in the composite peak, and the partial reduction of lead in $Pb(OH)_2$ to metallic lead (peak g). There are no peaks that could suggest the formation of indium sulfide similar to that reported in the case of $Bi_2S_3$-In film [4]. For this reason it is not possible to consider the reduction of lead from PbS. In the diffractograms of PbS + In films, with a thickness of PbS about 0.17 μm and annealed at 350 or 400°C, galena peaks reflection dominates over the metallic lead reflection. The presence of indium oxide peak in this diffractogram can not be distinguished as it overlaps with galena (200) peak.

Fig. 7 shows X-ray fluorescence (XRF) data on the relative intensity of lead, indium and sulfur in the as-prepared and nitrogen-annealed PbS + In films (0.14 + 0.02 μm). This analysis demonstrates that nitrogen-annealing process (up to 400°C) does not cause loss of lead, indium or sulfur in the films. And the noted changes in the relative intensity of the XRF signals for lead, indium and sulfur in as-prepared or annealed films can be explained as due to small differences in the thickness of the films. For this reason, we suppose that the presence of metallic lead peaks in the XRD diffractograms can just come from the $Pb(OH)_2$ in the film. The formation of indium sulfide could be another explanation about why there are no losses of indium or sulfur in the films. However, the absence of any indium sulfide peak in the XRD diffractograms does not support this hypothesis, unless an amorphous phase of $In_2S_3$ is the product of the solid state reaction.

The results of XRD and XRF studies, on the films, suggest that the formation mechanism of the composite
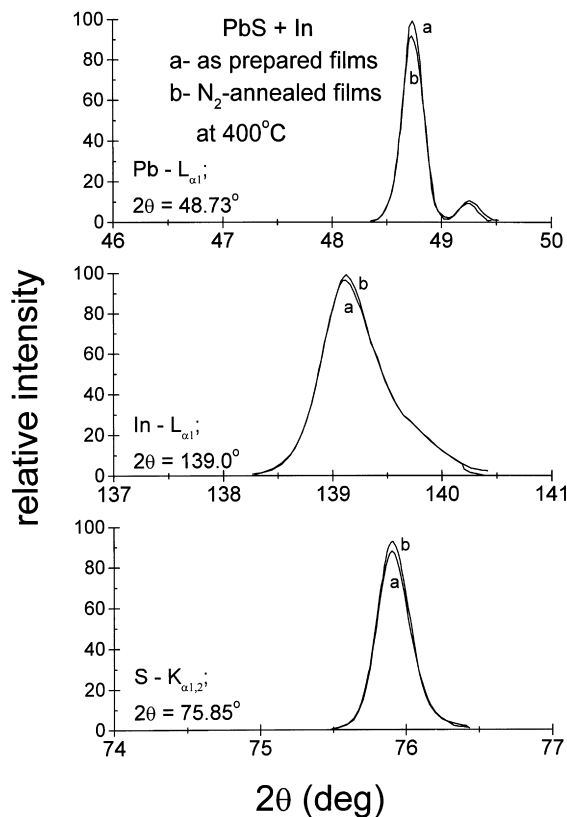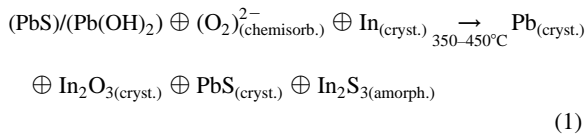
Fig. 7. X-ray fluorescence analysis in composite films: (a) as-prepared; and (b) nitrogen-annealed at 400°C.

film, from PbS + In film, can be represented as follows:

$$(PbS)/(Pb(OH)_2) \oplus (O_2)^{2-}_{(chemisorb.)} \oplus In_{(cryst.)} \xrightarrow[350-450°C]{} Pb_{(cryst.)}$$

$$\oplus In_2O_{3(cryst.)} \oplus PbS_{(cryst.)} \oplus In_2S_{3(amorph.)}$$

(1)

The amorphous nature of $In_2S_3$ ($III_2VI_3$) may be similar to those reported for ($V_2VI_3$) compound semiconductors such a $Bi_2S_3$ [18].

### 3.2. Optical transmittance spectra

The optical transmittance and specular reflectance spectra of PbS films as prepared and nitrogen-annealed at 350 and 400°C are shown in Fig. 8. For all these films, as common characteristic, the specular reflectance is higher than transmittance, which is in accordance, with that reported in [15,16] for PbS.

The optical transmittance and specular reflectance of as-prepared and nitrogen-annealed PbS + In films are shown in Fig. 9. In the as-prepared PbS + In films, the transmittance in the Vis region is near zero. In the NIR region, the transmittance is about 10–20%. The specular reflectance in the NIR region is about 60–70%. This

modification in the optical properties of the as-prepared PbS + In film, compared to that of the PbS film in Fig. 8, arises from the overlying indium film.

As we already mentioned, in Eq. (1), nitrogen-annealing process at 350 or 400°C of PbS + In films involves the reaction of metallic indium with available oxygen in the film to form indium oxide, metallic lead, an amorphous phase of $In_2S_3$ and residual quantities of PbS. The formation of the composite film substantially changes the original optical properties of PbS + In films. The conversion of metallic indium to $In_2O_3$, in the PbS + In film, leads to a substantial increment of the transmittance in the Vis and NIR region over the reflectance of these films, while in nitrogen-annealed single PbS films the specular reflectance dominates over the optical transmittance.

When we compare the transmittance of nitrogen-annealed PbS and PbS + In films in Figs. 8 and 9, it is noticed that the absorption edge of PbS + In films has been shifted to short wavelengths due to the presence of $In_2O_3$ and amorphous $In_2S_3$ components in the film.

For an approximate evaluation of energy gaps of PbS and composite films, we plotted the optical transmittance corrected for the reflection losses. Assuming that, the reflection loss is dominated by that at the air–film interface, the corrected optical transmittance can be given by
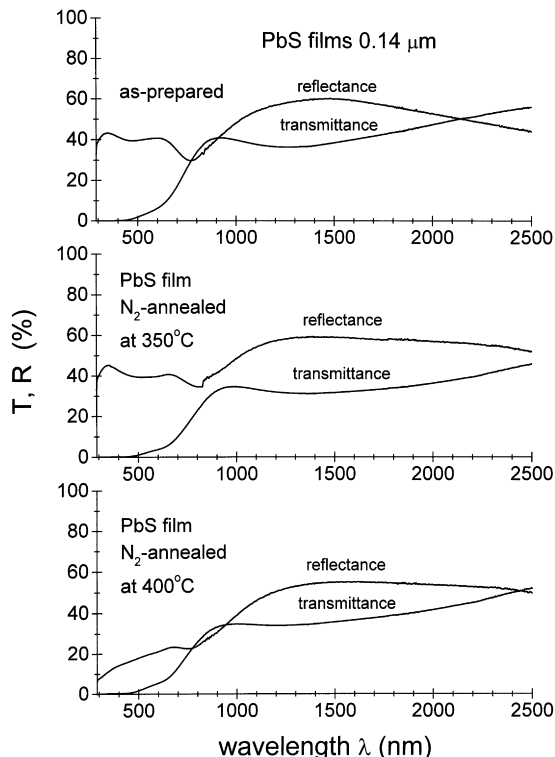


Fig. 8. Optical transmittance (*T*%) and specular reflectance (*R*%) spectra of PbS thin film as-prepared and nitrogen-annealed at 350 and 400°C.
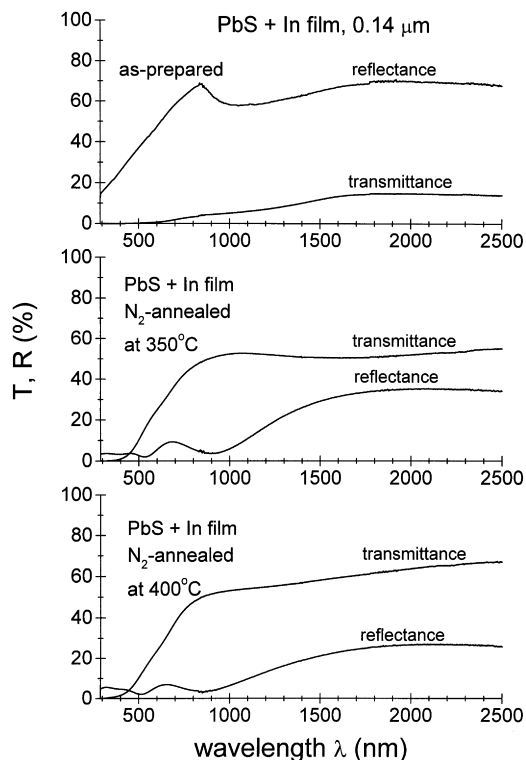
Fig. 9. Optical transmittance (T%) and specular reflectance (R%) spectra of PbS + In film as-prepared and nitrogen-annealed at 350 and 400°C.



Fig. 10. Plots of $[\alpha]^{1/2}$ versus h$\nu$ for PbS films annealed at 350 and 400°C.

$T_{\lambda(corr)}(\%) = 100*T_{\lambda}(\%)/100 - R_{\lambda}(\%)$. The corrected transmittance curves of PbS films demonstrates that the absorption edge is shifted to longer wavelengths, see Fig. 10. The optical energy gaps were calculated using $\alpha^{1/2}$ vs. h$\nu$, where $\alpha = (1/d)/\ln(100/T_{\lambda(corr)})$ in cm$^{-1}$ and h$\nu$ is the photon energy (eV), as applicable to indirect gap materials [19]. Fig. 10 shows the $\alpha^{1/2}$ vs. h$\nu$ plots of as-prepared and nitrogen-annealed PbS films at 350 and 400°C.

The indirect optical gap is about 0.7 eV for as-prepared PbS films. Upon annealing the film at 350 or 400°C in nitrogen, the band gap shifts from 0.4 to 0.45 eV range, which is in accordance to the indirect gap of 0.41 eV (300 K) reported for PbS [20]. The shift towards the high energy of the band gap, of as-prepared PbS films, should be due to quantum confinement of the charge carriers in the crystallites [21], as the size of the crystallites is about 10 nm (Table 1).

Since the composite films are formed by different components we expected to find a resultant band gap for the composite film. Fig. 11 shows the plots $\alpha^2$ vs. h$\nu$, where $\alpha = (1/d)/\ln(100/T_{\lambda(corr)})$ in cm$^{-1}$ for composite films. The energy gap was calculated from the corrected optical transmittance spectra of these films.

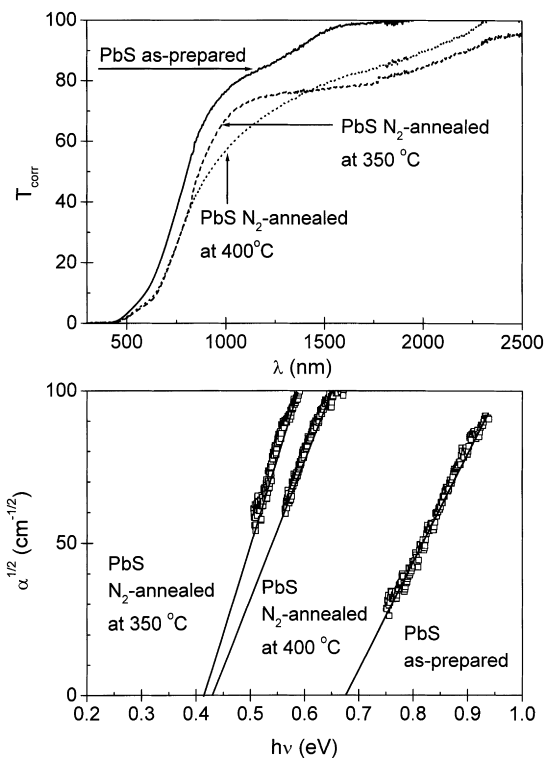The optical absorption in the composite film, formed in the present case, may be explained by means of a relatively high energy gap of 2.2–2.6 eV in the Vis–UV region and low energy gap of 0.6–0.7 eV in the NIR region. The observed high energy gap may result from the band gap 3.5 eV for In$_2$O$_3$ and >2.03 for amorphous In$_2$S$_3$ [20] and the low energy gap may be due to the PbS component. The transition of indirect to direct gap of the PbS component is not readily explained.

### 3.3. Electrical conductivity

Fig. 12 shows the photocurrent response curves of as-prepared and nitrogen-annealed PbS thin films. Photocarrier generation is notable only in the as-prepared PbS film. This film is formed by a mix of polycrystalline galena and possibly Pb(OH)$_2$ phase.

The nitrogen-annealed PbS films do not present photoconductivity and the dark current is about two orders higher as compared to as-prepared PbS films. The increase in the electrical conductivity of PbS films, after nitrogen-annealing, at 350 and 400°C, are attributed to improvement in the crystallinity of the film (Table 1).

Significant improvement in the electrical conductivity is observed in the case of nitrogen-annealed PbS + In films. The annealing process, of PbS + In films, changes the initial composition of the film and improves the electrical conductivity in almost five orders of magnitude as compared
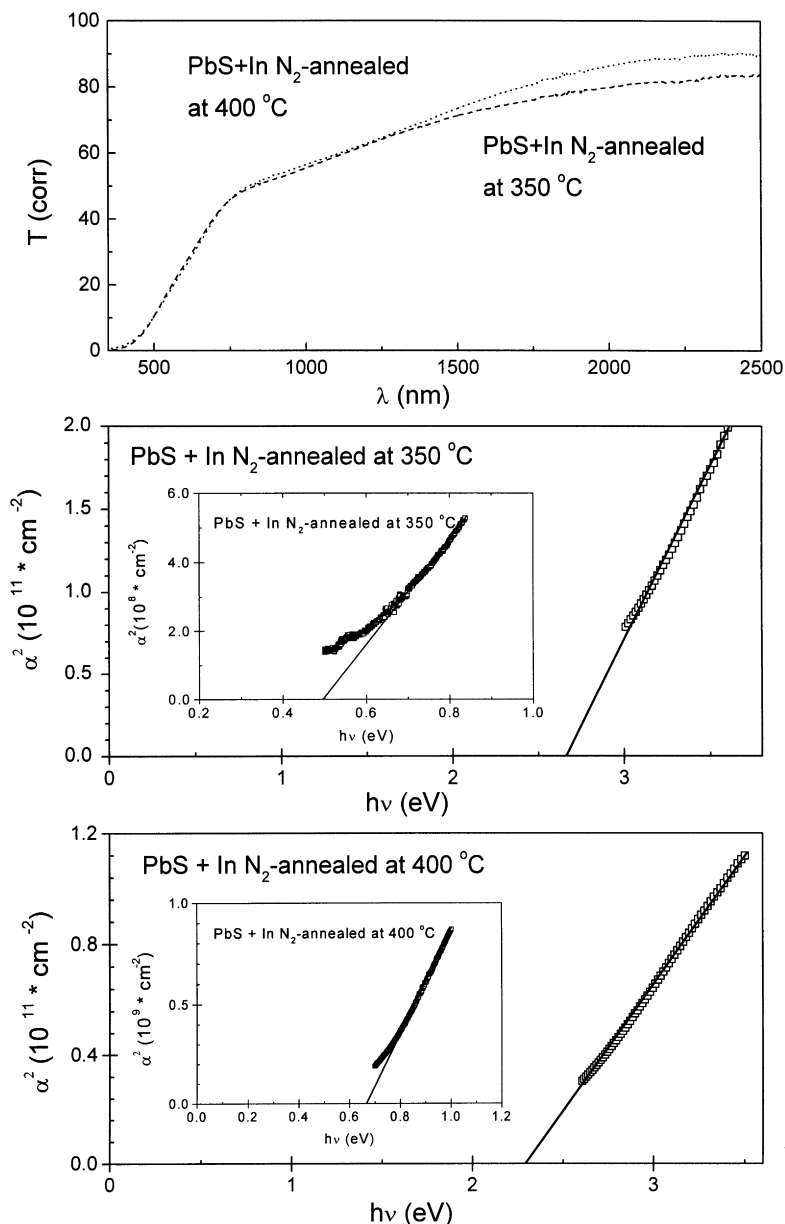
Fig. 11. Plots of $[\alpha]^2$ versus $h\nu$ for PbS + In films annealed at 350 and 400°C.

to as-prepared PbS films. The increment in the electrical conductivity of the composite films is related to a distribution of metallic lead particles in $In_2O_3/In_2S_3/PbS$ matrix. A hot probe thermoelectric test showed n-type conductivity for nitrogen-annealed PbS films and PbS + In films. The n-type conductivity was contemplated, in these films, from the composition of the type: $Pb_{1-x}S_{1-z}/Pb_x$ in the case of PbS, metallic lead and indium oxide in the case of nitrogen-annealed PbS + In films. The electrical conductivity of the composite film formed by nitrogen-annealing at 400°C, is about $10^3 \, \Omega^{-1} \, cm^{-1}$.

## 4. Conclusions

In the present work, we reported a method to produce an electrically conductive and optically absorbing composite film by annealing PbS + In film in nitrogen atmosphere at temperature above 300°C. Typical conductivity of the coating is $\sim 10^3 \, \Omega^{-1} \, cm^{-1}$.

XRD and XRF analysis on the composite film suggested that it contains PbS, Pb, $In_2O_3$ and $In_2S_3$ components.

This work supplements earlier results on chemically deposited CdS + In, CdSe + In and In + $Bi_2S_3$ films.
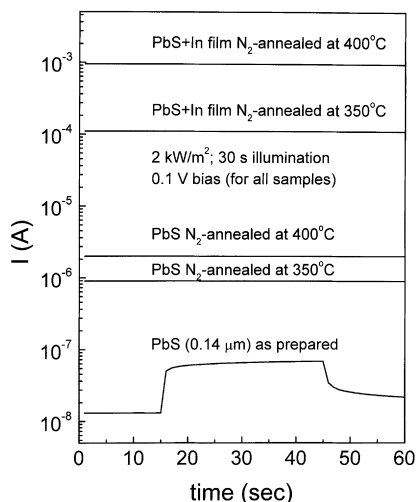
Fig. 12. Photocurrent response curves of the as-prepared and nitrogen-annealed PbS and PbS + In films at 350 and 400°C.

Results presented here confirm that chemical deposition technique may be combined with thermal evaporation of metallic films to produce coatings with modified electrical and optical properties.

## Acknowledgements

## References

[1] P.G. George, A. Sánchez, P.K. Nair, M.T.S. Nair, Appl. Phys. Lett. 66 (1995) 3624–3626.

[2] V.M. García, P.J. George, M.T.S. Nair, P.K. Nair, J. Electrochem. Soc. 143 (9) (1996) 2892–2895.

[3] P.J. George, A. Sánchez, P.K. Nair, L. Huang, J. Cryst. Growth 4055 (1995) 1–8.

[4] R. Suárez Parra, P.J. George, A.E. Jiménez-González, L. Baños, P.K. Nair, J. Solid State Chem. 138 (2) (1998) 290–296.

[5] A.N. Kovalev, V.V. Korablev, Thin Solid Films 161 (1988) 281–287.

[6] T.K. Chaudhuri, H.N. Acharya, B.B. Nayak, Thin Solid Films 83 (1981) 169–172.

[7] T.K. Chaudhuri, Int. J. Energy Res. 16 (1992) 481–487.

[8] T.K. Chaudhuri, S. Chatterjee, Int. Conf. on Thermoelec. Arlington, USA, October, 1992, pp. 7–9.

[9] S. Chatterjee, T.K. Chaudhuri, H.N. Acharya, Int. Conf. on Thermoelec., Arlington, USA, October (1992) 7–9.

[10] N.C. Sharma, D.K. Pandya, H.K. Sehgal, K.L. Chopra, Thin Solid Films 62 (1979) 97–108.

[11] V. Reddy, D.K. Dutta, K.L. Pandya, Solar Energy Mater. 5 (1981) 187–197.

[12] P.K. Nair, M.T.S. Nair, Semicond. Sci. Technol. 4 (1989) 807–814.

[13] R. Suárez Parra, P.K. Nair, J. Solid State Chem. 123 (1996) 296–300.

[14] P.K. Nair, M.T.S. Nair, V.M. García, O.L. Arenas, Y. Peña, A. Castillo, I.T. Ayala, O. GomezDaza, A. Sánchez, J. Campos, H. Hu, R. Suárez, M.E. Rincón, J. Solar Energy Mater. Solar Cells 52 (1998) 313–344.

[15] P.K. Nair, M.T.S. Nair, J. Phys. D: Appl. Phys. 23 (1990) 150–155.

[16] R.A. Zingaro, D.O. Skovlin, J. Elechtrochem. Soc. 111 (1964) 42.

[17] B.D. Cullity, Elements of X-ray Diffraction, 2, Addison-Wesley, Reading, MA, 1978.

[18] M.E. Rincón, R. Suárez, P.K. Nair, J. Phys. Chem. Solids 57 (2) (1996) 1947–1955.

[19] K.V. Shalimova, Fisica de los semiconductores, Mir, Moscow, 1975, pp. 264–275.

[20] O. Madelung (Ed.), Semiconductors: Other than Group IV Elements and III–V Compounds Springer, Berlin, 1992.

[21] R. Vogel, P. Hoyer, H. Weller, J. Phys. Chem. 98 (12) (1994) 3183–3188.